Functional Materials 19, No.2 (2012) 

# Laser characteristics of $NaLa(MoO_4)_2:Nd^{3+}$ and $NaLa(Mo_{0.5}W_{0.5}O_4)_2:Nd^{3+}$ crystals

*A.N.Shekhovtsov*

Institute for Single Crystals, STC "Institute for Single Crystals", National Academy of Sciences of Ukraine, 60 Lenin Ave., 61001 Kharkiv, Ukraine

*Received November 19, 2011*

Pure and $Nd^{3+}$-doped $NaLa(Mo_{0.5}W_{0.5})_2$ and $NaLa(MoO_4)_2$ single crystals have been grown by the Czochralski technique. Their laser characteristics have been defined and analyzed.

Методом Чохральского выращены чистые и активированные $Nd^{3+}$ монокристаллы $NaLa(Mo_{0,5}W_{0,5})_2$ и $NaLa(MoO_4)_2$. Определены и проанализированы их лазерные характеристики.

## *1. Introduction*

Interest to the problems bound up with the obtaining of tungstate and molybdate crystals with "sheelite" structure and the study of their properties is caused by the fact that they are promising in the capacity of active media which use the effect of stimulated Raman scattering (SRS).

The group of such crystals includes not only tungstates and molybdates of alkali earth elements and lead for which laser generation and SRS conversion have been achieved, but also tetragonal crystals of binary tungstates and molybdates $MLn(WO_4)_2$ and $MLn(MoO_4)_2$, where M and Ln are alkali metal and rare-earth elements, respectively. These crystals are characterized by structural disorder: in their crystal lattice the cations are statistically distributed in zigzag chains along the axis *c*, due to close values of ionic radii of alkali and rare-earth cations. Statistical cation distribution is observed at $R_{ion}(M^+)/R_{ion}(Ln^{3+}) < 1.27$, whereas for $R_{ion}(M^+)/R_{ion}(Ln^{3+}) > 1.32$ the distribution is ordered [1]. The internal vibrations of the anionic complex are sensitive to the local surrounding, therefore in the ordered structure there are observed splitting of the vibration modes and rise of the intensity of the RS lines. For the binary tungstates and molybdates the shift of the frequency is ~920 $cm^{-1}$ and ~890 $cm^{-1}$, respectively [1].

$MLn(WO_4)_2$ and $MLn(MoO_4)_2$ crystals doped with $Ln^{3+}$ ($Nd^{3+}$, $Tm^{3+}$, $Yb^{3+}$, $Er^{3+}$) ions show spectroscopic and generation characteristics promising for practical use [2–7]. For such crystals widening of the spectral lines of the activators is nonuniform [8]. This gives an advantage for diode pumping. The generation efficiency at different types of pumping runs into 40 %.

For the first time the laser characteristics of $NaLa(MoO_4)_2:Nd^{3+}$ (NLMO) crystal at flash-lamp pumping were reported in [9], however, due to low thermophysical characteristics of the crystal the obtained data did not attract much attention. Nowadays interest to NLMO doped with RE is explained by the prospects of their use in diode-pumped Raman lasers in which the active laser medium also functions as the Raman converter [10]. This allows to extend the spectral range of $NaLa(MoO_4)_2:Nd^{3+}$ laser due to the Raman scattering, by obtaining additional generation lines shifted with respect to the basic generation line of $Nd^{3+}$ ($\lambda = 1.06$ μm, the transition $^4F_{3/2} \rightarrow {}^4I_{11/2}$) by the values $\nu_{R1} = 888$ $cm^{-1}$ and $\nu_{R2} = 320$ $cm^{-1}$, corresponding to the symmetric vibrational optical modes of the

Table 1. Crystal growth conditions and concentrations of uncontrolled impurities

| Crystal | Atm. | Dopant | $C_{Nd}$, mass.% | Growth conditions | | |
|---|---|---|---|---|---|---|
| | | | | $dT/dz$, °C/cm | V, mm/h | ω, rot.$^{-1}$ |
| $NaLa(MoO_4)_2$ | air | $NaNd(MoO_4)_2$ | 0.6 | 40–60 | 2–5 | 20–30 |
| $NaLa(Mo_{0.5}W_{0.5}O_4)_2$ | $N_2$ | $NaNd(MoO_4)_2$ | 0.3 | 50–70 | 2–5 | 15–30 |
| Impurities, mass.% | | | | | | |
| $NaLa(MoO_4)_2$ | Fe — $7\cdot10^{-4}$; Cu — $1\cdot10^{-4}$; Al — $1\cdot10^{-4}$; Mg — $1\cdot10^{-4}$; W — $1\cdot10^{-3}$; Pb — $2\cdot10^{-4}$ | | | | | |
| $NaLa(Mo_{0.5}W_{0.5}O_4)_2$ | Fe — $6\cdot10^{-4}$; Cu — $1\cdot10^{-4}$; Al — $2\cdot10^{-4}$; Mg — $2\cdot10^{-4}$; Pb — $3\cdot10^{-4}$ | | | | | |

tetrahedral complex $(MoO_4)^{2-}$. Efficient SRS generation was obtained for NLMO crystal possessing two SRS-active vibrational modes 888 and 320 cm$^{-1}$ pumping with YAG:$Nd^{3+}$ [11]. More than 50 % of the pumping power were distributed into the Stokes and anti-Stokes components. At flash-lamp pumping of $KLa(MoO_4)_2$:$Nd^{3+}$ and NLMO:$Nd^{3+}$ crystals the authors of [12] obtained ~40 % generation efficiency of the first Stokes component with a pulse duration of 1.2 – 2.5 ps. These results make it possible to assume that crystalline $MLn(WO_4)_2$ and $MLn(MoO_4)$ matrices are promising nonlinear active media for laser facilities working in the near IR region. The use of $LaNa(Mo_{1-x}W_xO_4)_2$ solid solution crystals will allow to shift the $Nd^{3+}$ generation frequency on the vibrational modes of both $(MoO_4)^{2-}$ and $(WO_4)^{2-}$ cations.

The active elements of the Raman lasers must possess high generation efficiency and high damage threshold, since efficient generation of the Stokes components requires higher pumping powers. Simultaneous laser generation and efficient Raman conversion can be achieved in the crystals with high structure perfection (not containing impuritiy phase inclusions, color centers, etc.). This can hardly be realized for lead tungstate and molybdate SRS crystals consisting of several elements which charge state may vary (Pb, W, Mo). Moreover, introduction of the ions ($Nd^{3+}$, $Yb^{3+}$) necessitates the use of co-activator ions, or realization of the mechanism of excessive charge compensation of vacancy type. At doping with $Nd^{3+}$ and $Yb^{3+}$ this may result in essential spread of the frequencies and decrease of the intensity of the RS lines. As a consequence, the efficiency of radiation conversion will diminish.

In view of the above-said, it is of considerable interest to grow the crystals possessing high level of doping, as well as to study their spectral, kinetic and laser characteristics (generation efficiency and damage threshold).

## 2. Experimental

The starting material for the growth of pure NLMO and doped $LaNa(Mo_{0.5}W_{0.5}O_4)_2$ (NLMWO) crystals was prepared by the method of solid phase synthesis using high-purity $La_2O_3$, $WO_3$ and $Na_2CO_3$ as well as analytically pure $MoO_3$. The mixture of the initial components taken in the stoichiometric ratio was subjected to thermal treatment in air at 750°C during 5 h. The resulting compound was formed according to the reaction:

$$Na_2CO_3 + La_2O_3 + 4MoO_3 \rightarrow \rightarrow 2LaNa(MoO_4)_2 + CO_2\uparrow. \quad (1)$$

The crystals were grown onto a seed oriented along the direction [001] by the Czochralski method using the automated setup "Analog" with crystal weight control. The growth process was realized in platinum crucibles with a volume of 200 cm$^3$. The growth parameters for all the crystals were the following: the pulling rate equaled 1 – 3 mm/h, the rotation rate was 15 – 30 min$^{-1}$, the temperature gradient being 40 – 70 deg./cm. $Nd^{3+}$ doping was carried out by means of $NaNd(MoO_4)_2$ compound. The crystals had a diameter up to 35 mm and a length up to 60 mm. All the grown samples did not contain impurity phases and macro-inclusions (bubbles, cracks, etc.).

Pure and doped NLMO crystals grown in nitrogen atmosphere were practically black, with a very low transmission in the visible and near-IR regions. Such a color seems to be caused by the formation of color centers bound up with the reduction of molybdenum to "+5". Analogous results were obtained in [13], at the growth of NLMO:Er,Ce crystals in argon atmosphere. Therefore, we chose oxygen-containing medium. Pure NLMO crystals grown in this atmosphere had a weak yellow color characteristic of most

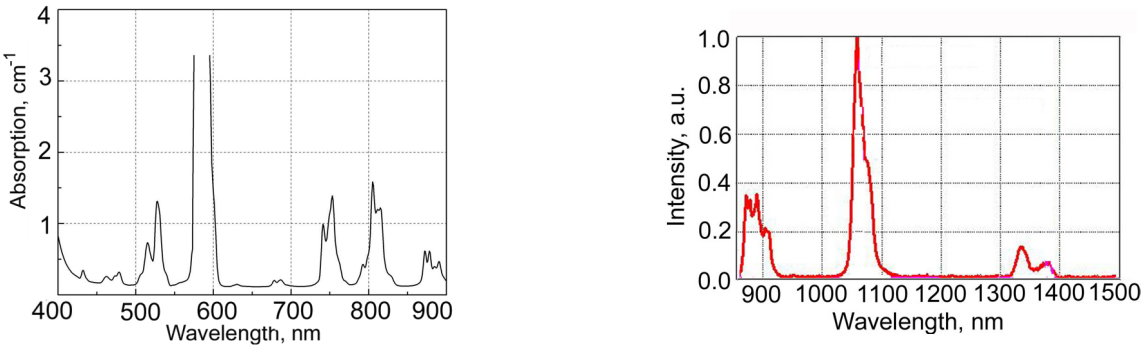


Fig. 1. Absorption (a) and luminescence (b) spectra of $LaNa(MoO_4)_2:Nd^{3+}$ crystal.

molybdates. The neodymium containing NLMO crystals were lilac.

The concentrations of uncontrolled impurities in NLMO and NLMWO crystals is shown in Table 1. As is seen, in both crystals the total concentration of uncontrolled impurities does not exceed $2 \cdot 10^{-3}$ mass. %.

The absorption spectra were studied in 190 – 1100 nm range using a two-beam spectrophotometer of Perkin-Elmer type, the luminescence spectra were obtained by means of a MDP-204 monochromator. Luminescence decay in the studied samples was measured by a tunneling laser based on LiF crystal with the color centers $F_2^+$ ($\lambda$ = 890 – 1050 nm) pumped by the second harmonic of $GGG:Nd^{3+}$ laser ($\lambda$ = 531 nm).

The generation characteristics were tested by means of a tuned alexandrite laser $Al_2O_3:BeO:Cr^{3+}$ with flash-lamp pumping, and a pulse output energy up to 300 mJ. Thereat, the generation pulse duration was 50 μs, the pulse repetition frequency being 5 – 10 Hz.

The damage threshold was measured using a $YAG:Nd^{3+}$ laser ($\lambda$ = 1.06 μm, $TEM_{00}$ mode, 1 Hz pulse repetition frequency, 10 ns pulse duration, the spot diameter was 45 μm, the Gaussian distribution of the intensity. The samples with the dimensions 10×10×10 $mm^3$ were cut out from the cylindrical part of the crystal and oriented along all the crystallographic directions.

### 3. Results and discussion

The crystalline structure of NLMO crystals consist of a three-dimensional skeleton formed by zigzag like chains of lanthanum and sodium polyhedrons. The lanthanum and sodium cations are coordinated by eight oxygen atoms, for tungsten (molybdenum) the quantity of these atoms is four. The lanthanum and sodium polyhedrons are joined and form spirals around [001]. In this crystalline structure the sodium and lanthanum cations are statistically distributed in the chains. Since the difference between the ionic radii of $La^{3+}$ (1.06 Å) and $Nd^{3+}$ (0.99 Å) is very small, $Nd^{3+}$ may be also distributed in the chains.

The absorption and luminescence spectra of $NLMO:Nd^{3+}$ and $NLMWO:Nd^{3+}$ crystals are identical. In the region of $\lambda$ = 400 – 900 nm the absorption spectra (Fig. 1a) contain the lines characteristic of the transitions $f - f$ of $Nd^{3+}$ ion. In the regions of 850 – 950 nm, 1040 – 1100 nm and 1320 – 1400 nm there is observed luminescence corresponding to the radiative transitions ${}^4F_{3/2} \rightarrow {}^4I_{9/2,\ 11/2,\ 13/2}$ of $Nd^{3+}$ ion (Fig. 1b). These data coincide with the ones reported in [14], where the scheme of the energy levels for the lowest terms of $Nd^{3+}$ ion in NLMO is built.

For both $NLMO:Nd^{3+}$ and $NLMWO:Nd^{3+}$ crystals the decay kinetics of the metastable level ${}^4F_{3/2}$ of $Nd^{3+}$ ion ($\lambda$ = 1065 nm) measured at room temperature is monoexponential, the decay times are 180 and 165 μsec, respectively (Fig. 2).

Alexandrite laser makes it possible to simulate the regime of diode pumping with rather high (5 – 10 Hz) pulse repetition frequency, pumping pulse energy exceeding the one of diode laser and wide ($\lambda$ = 710 – 775 nm) range wavelength tunnig. For pumping of the investigated crystals the wavelength of alexandrite laser was tuned to $\lambda$ = 752 nm in accordance with one of the maxima of $Nd^{3+}$ absorption spectrum in NLMO and NLMWO crystals.

In the process of pumping by pulsed alexandrite laser we obtained generation of $Nd^{3+}$ ions in NLMO crystal at 1.065 and 1.382 μm wavelengths. The differential efficiency of laser generation at the funda-

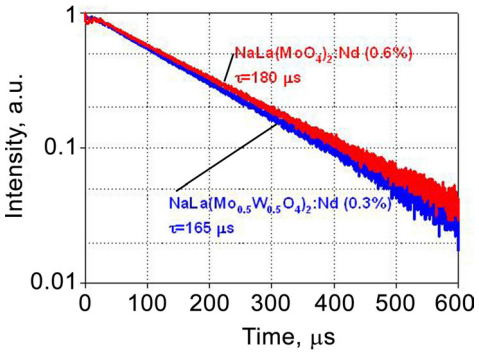


Fig. 2. Decay time of metastable $^4F_{3/2}$ level ($\lambda = 1064$ nm) in $LaNa(W_{0.5}Mo_{0.5}O_4)_2:Nd^{3+}$ and $LaNa(MoO_4)_2:Nd^{3+}$ crystals.

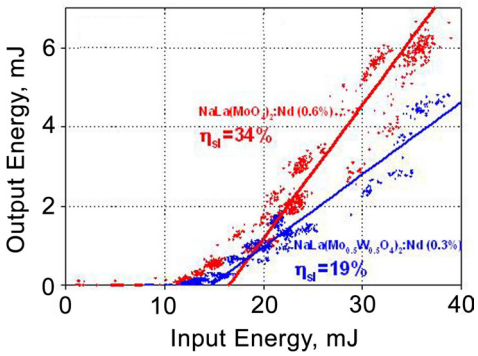


Fig. 3. Dependence of laser output energy upon pumping energy for $LaNa(W_{0.5}Mo_{0.5}O_4)_2:Nd^{3+}$ and $LaNa(MoO_4)_2:Nd^{3+}$ crystals.

mental wavelength 1.065 μm run into 34 % with respect to the absorbed pumping energy (Fig. 3). $NLMWO:Nd^{3+}$ solid solution showed 19 % (i.e. approximately half as high) efficiency of laser generation at $\lambda = 1.065$ μm (Fig. 3). The generation thresholds for both crystals had close values: 16.7 and 13.7 mJ, respectively.

As is known, the radiation strength of crystalline matrix is defined by its structure perfection, i.e. the presence of impurity phases (which, as a rule, are located at the block boundaries), inhomogeneity of the crystal composition, the presence of activator centers and structure defects [15]. The latter may sharply raise the absorption of laser pulse energy, accumulation of mechanical stresses and, as a consequence, lead to destruction of the material.

It is known [16] that some impurities may essentially increase the radiation strength of crystals. This is caused by different factors, in particular, formation of electron capture centers which raises the threshold of electron avalanche formation; prevention of the formation of the defects critical for optical breakdown; change of the mechanical characteristics. Therefore, we studied the influence of $Nd^{3+}$ on the damage threshold of the binary tungstate, molybdate and its solid solution (Table 2). For comparison, this table contains the data on the damage threshold of high-efficiency SRS-crystals $PbMoO_4$:Nd, $PbWO_4$:Nd and $KGd(WO_4)_2$:Nd measured under the same conditions; for these crystals simultaneous laser generation and SRS conversion have been obtained [17]. The concentration dependence of the radiation strength of NLMO:Nd and NLMWO:Nd crystals was not studied.

As seen from Table 2, the maximum value of optical breakdown (104 J/cm$^2$) is

Table 2. Damage threshold of $LaNa(W_{0.5}Mo_{0.5}O_4)_2$ and $LaNa(MoO_4)_2$ crystals

| | $J_{Th}$, J/cm$^2$ | |
|---|---|---|
| | Pure | Nd — doped; (wt.%) |
| $NaLa(MoO_4)_2$ | 104 | 29; (0.6) |
| $NaLa(Mo_{0.5}W_{0.5}O_4)_2$ | 42 | 51; (0.3) |
| $KGd(WO_4)_2$ | | 55; (0.98) |
| $PbMoO_4$ | 58 | 90; (0.75) |
| $PbWO_4$ | 10 | 52; (0.7) |

observed in pure NLMO crystal, whereas the $Nd^{3+}$ doping diminishes the radiation strength to 29 J/cm$^2$. For NLMWO solid solution crystal the presence of neodymium ions practically does not influence the radiation strength. Its value is on the level with the one for $PbWO_4$:Nd and $KGd(WO_4)_2$:Nd crystals.

## 4. Conclusions

The obtained generation efficiency and radiation strength of NLMO:Nd crystal and its solid solution are close to those of the best representatives of SRS-crystals, such as the "commercial" $KGd(WO_4)_2$:Nd for which the growth technology and activator concentration are optimized, and $PbMoO_4$:Nd [18]. Further investigations aimed at upgrading the technology of the growth of these crystals and optimization of the activator concentration will make it possible to improve their functional characteristics and trigger off practical application of dielectric single-crystalline media in the facilities based on the use of SRS.

Author is grateful to Mr.B.P.Nazarenko, Prof.M.B.Kosmyna, Dr.A.V.Lopin and Dr.M.E.Doroshenko (GPI RAN) for experiments and helpful discussion during the preparation of manuscript.

### *References*

1. B.A.Kolesov, L.P.Kozeeva, *Zh.Strukt. Khimii*, **34**, 52 (1993).
2. A.Garcia-Cortes, C.Cascales, A.de Andres et al., *IEEE J.Quant. Electr.*, **43**, 157 (2007).
3. A.A.Kaminskii, H.J.Eichler, Ken-ichi Ueda et al., *Appl. Opt.*, **38**, 4533 (1999).
4. E.V.Zharikov, D.A.Lis, A.M.Onischenko et al., *Kvant. Elektron.*, **36**, 39 (2006).
5. K.A.Subotin, E.V.Zharikov, V.A.Smirnov, *Opt. i Spektr.*, **92**, 657 (2002).
6. E.V.Zharikov, D.A.Lis, A.V.Popov et al., *Kvant. Elektr.*, **36**, 515 (2006).
7. T.T.Basiev, M.E.Doroshenko, Yu.N.Gorobets et al., Abstract book of "ICCM-2007"Kharkov, Ukraine B1 (2007).
8. Yu.K.Voron'ko, A.A.Sobol, S.N.Ushakov, V.E.Shukshin, *Neorgan. Mater.*, **38**, 478 (2002).
9. A.A.Kaminskii, G.Ya.Kolodnyi, N.I.Sergeeva, *Zh. Prikl. Spektr.*, **IX(5)**), 884 (1968).
10. T.T.Basiev, V.V.Osiko, *Uspekhi Khimii*, **75**, 939 (2006).
11. A.A.Kaminskii, S.N.Bagaev, D.Grebe et al., *Kvant. Elektr.*, **23**, 199 (1996).
12. K.Andrunas, Yu.Vischakas, V.Kabelka et al., *Pisma v Zh. Eksper. Teor. Fiz.*, **42**, 333 (1985).
13. G.M.Kuzmicheva, E.V.Zharikov, K.A.Subotin et al., *Neorg. Mater.*, **41**, 1133 (2005).
14. A.M.Morozov, M.N.Tolstoy, P.P.Feofilov, V.N.Shapovalov, *Opt. i Spectr.*, **22**, 414 (1967).
15. A.A.Manenkov, A.M.Prokhorov, *Uspekhi Phiz. Nauk*, **148**, 179 (1986).
16. P.A.Thomas, B.E.Walts, *Solid State Commun.*, **73**, 97 (1990).
17. T.T.Basiev, V.N.Baumer, Yu.N.Gorobets et al., *Cryst. Reports*, **54**, 697 (2009).
18. T.T.Basiev, M.E.Doroshenko, L.I.Ivleva et al., *Kvant. Elektr.*, **36**, 720 (2006).

## Лазерні характеристики кристалів $NaLa(MoO_4)_2:Nd^{3+}$ та $NaLa(Mo_{0.5}W_{0.5}O_4)_2:Nd^{3+}$

***О.М.Шеховцов***

Методом Чохральського вирощено чисті та активовані $Nd^{3+}$ монокристали $NaLa(Mo_{0,5}W_{0,5})_2$ та $NaLa(MoO_4)_2$. Визначено та проаналізовано їх лазерні характеристики.